JOURNAL OF MATERIALS SCIENCE 21 (1986) 1368–1376

# Superplastic deformation of Al–Li–Cu–Mg alloy sheet

A. J. SHAKESHEFF, P. G. PARTRIDGE
*Materials and Structures Department, Royal Aircraft Establishment, Farnborough, Hants, UK*

Al–2.5 Li–1.2 Cu–0.6 Mg–0.12 Zr (wt%) alloy sheet was cold-rolled, solution heat-treated for 20 min at 510° C, prestrained by 3% and superplastically deformed at 450 to 540° C at strain rates between $1 \times 10^{-4}$ and $2.8 \times 10^{-1}$ $sec^{-1}$. The maximum elongation obtained was 300%. Significant cavitation occurred above about 0.5 strain at a rate (void volume/unit strain) of 4% at 540° C and 6% at 500° C. The onset of cavitation coincided with a reduction in the room-temperature tensile properties after reheat-treatment. During annealing at 500 to 540° C, grain coarsening near the sheet surface was associated with magnesium and lithium depletion. Superplastic deformation produced a fine equiaxed microstructure by dynamic recrystallization.

## 1. Introduction

Superplastic forming can be an attractive fabrication method for the production of complex components from aluminium and titanium alloy sheets, and substantial cost and weight savings compared with conventional fabrication techniques are predicted for aerospace components [1–4]. Unlike titanium alloys, aluminium alloys are prone to cavitation during superplastic deformation, and the cavitation can affect the mechanical properties [5–8]. Nevertheless, the use of superplastically formed aluminium alloys for aerospace application is increasing.

The effects of superplastic deformation on the microstructure and tensile properties of high strength Al–Zn–Mg alloys have been reported [6–9]. Although elongations up to 650% were obtained in these alloys the onset of cavitation occurred at elongations between 60 and 100%.

Aluminium alloys containing lithium are of special interest because of their lower density and high specific stiffness [10]. Direct replacement of components fabricated in currently available 2000 and 7000 Series alloys by aluminium alloys containing ~2.5% Li may result in weight savings of ~10%. Even greater weight savings might be achieved if these alloys could be superplastically formed.

This paper describes the superplastic behaviour of an Al–Li–Cu alloy provisionally specified DTDXXXA [11]. The effects of superplastic strain on the tensile properties are described and comparisons are made with the properties reported for Al–Zn–Mg type alloys.

## 2. Experimental techniques

The alloy had a composition (wt%) of Al–2.5 Li–1.2 Cu–0.6 Mg–0.12 Zr–0.2 Fe–0.15 Si and was supplied as 100 mm plate. This was rolled at 475° C to 65 mm and longitudinally cold-rolled to 1.6 mm. The sheet was then solution heat-treated for 20 min at 510° C, cold-water quenched and prestrained by 3%.

Microstructural studies were made on sheet in the as-received condition and after solution treatment at 500 and 540° C for times up to 24 h, followed by cold-water quenching. The microstructures after solution treatment were compared with those produced after superplastic deformation. The mean linear intercept grain size was determined in sections mechanically polished and etched in Kellers Reagent* at × 250 magnification, using a minimum of 40 lines, each 100 mm long and parallel to the principal directions in the sheet.

Electron probe microanalysis was carried out on some sections before and after annealing. Only magnesium X-ray counts per second were measured and these were proportional to the magnesium content, assuming that lithium and magnesium loss occurred and there was no further loss of other elements.

High-temperature tests were carried out in air at constant crosshead speed at temperatures of 450, 475, 500 and 540° C controlled to within ± 2° C over a zone 100 mm long. At the end of each test the furnace was raised, and the testpiece unloaded and air-cooled to room temperature within 2 to 3 min.

The test piece gauge length was 25 mm × 5 mm. Stepped strain-rate tests [7] were used to determine the strain rate sensitivity index $m$ given by

$$m = \frac{\log(\sigma_A/\sigma_B)}{\log(\dot{\varepsilon}_A/\dot{\varepsilon}_B)}$$

where $\sigma$ and $\dot{\varepsilon}$ are the true stress and true strain rate, respectively. Each test piece was given 0.03 pre-strain at an initial strain rate of $3.4 \times 10^{-4}$ $sec^{-1}$ before reducing the strain rate to $3.4 \times 10^{-5}$ $sec^{-1}$. The crosshead speed was then doubled from $\dot{\varepsilon}_A$ to $\dot{\varepsilon}_B$ after successive increments of 0.06 strain up to 50% strain.

Constant crosshead speed tests were carried out to

*Kellers Reagent: 2 ml 48% HF, 3 ml HCl, 5 ml conc. $HNO_3$, 190 ml $H_2O$.



0022–2461/86 $03.00 + .12 

determine the true stress–true strain curves (assuming constancy of volume) and total elongation to failure. During several of these tests, $m$ values were also determined after various strains by doubling the crosshead speed for a small increment of strain before reverting back to the original speed.

After superplastic strain, cavitation data were obtained by measuring the density of the gauge lengths and of the undeformed head regions of test pieces. Details of the procedures are described elsewhere [7].

To measure the effect of superplastic deformation at 500 and 540° C on the room-temperature tensile properties, longitudinal test pieces were superplastically deformed to strains between 0.1 and 0.9 and without further machining were solution heat-treated for 20 min, cold-water quenched, aged at 170° C for 60 h and air-cooled. Comparisons were made with undeformed longitudinal test pieces solution-treated at 500 and 540° C for equivalent superplastic deformation times and re-solution treated and aged prior to testing at room temperature.

An indication of the anisotropy of the superplastic deformation was obtained by measuring the plastic strain ratio $R$ after various superplastic strains, where

$$R = \frac{\ln(\omega_0/\omega_f)}{\ln(t_0/t_f)}$$

and $\omega_0$, $\omega_f$ and $t_0$, $t_f$ are the initial and final width and thickness, respectively, in the gauge length.

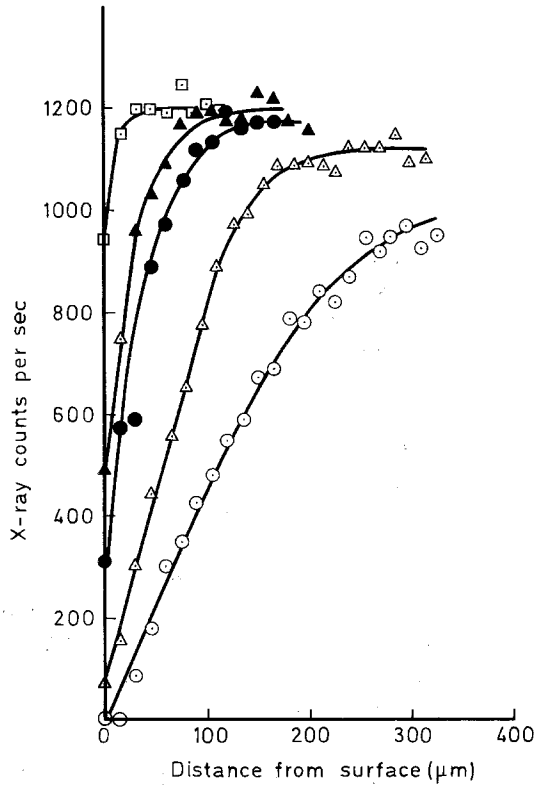


*Figure 1* Effect of time at temperature on the magnesium X-ray counts. (□) Prior to heat treatment, (▲) 3 h 500° C, (△) 24 h 500° C, (●) 3 h 540° C, (○) 24 h 540° C. All heat treatments followed by cold-water quench.

## 3. Results

### 3.1. Effect of solution treatment on microstructure

Shear bands persisted after solution treatment times up to 24 h at 500 and 540° C. During solution treatment a coarse-grained surface layer was produced. The layer thicknesses after 3 and 24 h at 500° C were 12 and 28 μm, respectively, and at 540° C they were 80 and 300 μm, respectively. Electron probe microanalysis revealed magnesium depletion in these layers, and the depletion increased with increase in the solution time and temperature (Fig. 1). The depths of magnesium depletion at 500° C after 3 and 24 h were 80 and 170 μm, respectively, compared with 90 and > 300 μm respectively, at 540° C.

### 3.2. Elevated temperature tests

The effects of test temperature and test-piece orientation on the true stress–true strain rate curves obtained from stepped strain-rate tests are shown in Fig. 2. The slope of the curve increased and the flow stress decreased with increase in temperature. The flow stress was lower in the longitudinal (L) direction, the rolling direction, than in the transverse (T) direction.

The effect of initial strain rate ($\dot{\varepsilon}_I$) and test temperature on the true stress–true strain curves for the L and T directions are shown in Fig. 3. The relative flow stresses in the T and L directions at strains less than 0.7 were the same as determined from stepped strain-rate tests. Peak $m$ values were similar (0.39 to 0.47) in both test directions, but at 500° C the peak value occurred at a higher strain rate in the L direction than in the T direction. The maximum value of $m$ tended to increase with increase in temperature. The effect of superplastic strain on $m$ is indicated in Fig. 3. The $m$ values obtained at 500° C were similar to those obtained in stepped strain-rate tests and the values increased with increase in strain.

The effects of test temperature, initial strain rate and test-piece orientation on total elongation are shown in Table I. The elongation values were greater in the L direction than in the T direction. Examples of L and T direction test pieces after superplastic strain are shown in Fig. 4. The greatest elongation obtained in the current tests was 300% in the longitudinal

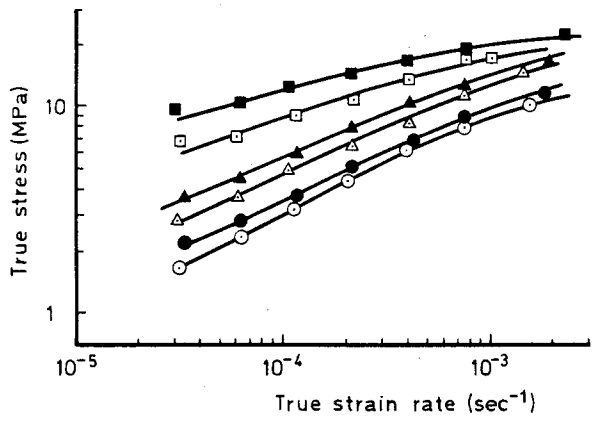


*Figure 2* True stress–true strain rate curves derived from stepped strain-rate tests. Open symbols, L test direction; closed symbols, T direction. (□, ■) 450° C; (△, ▲) 500° C; (○, ●) 540° C.

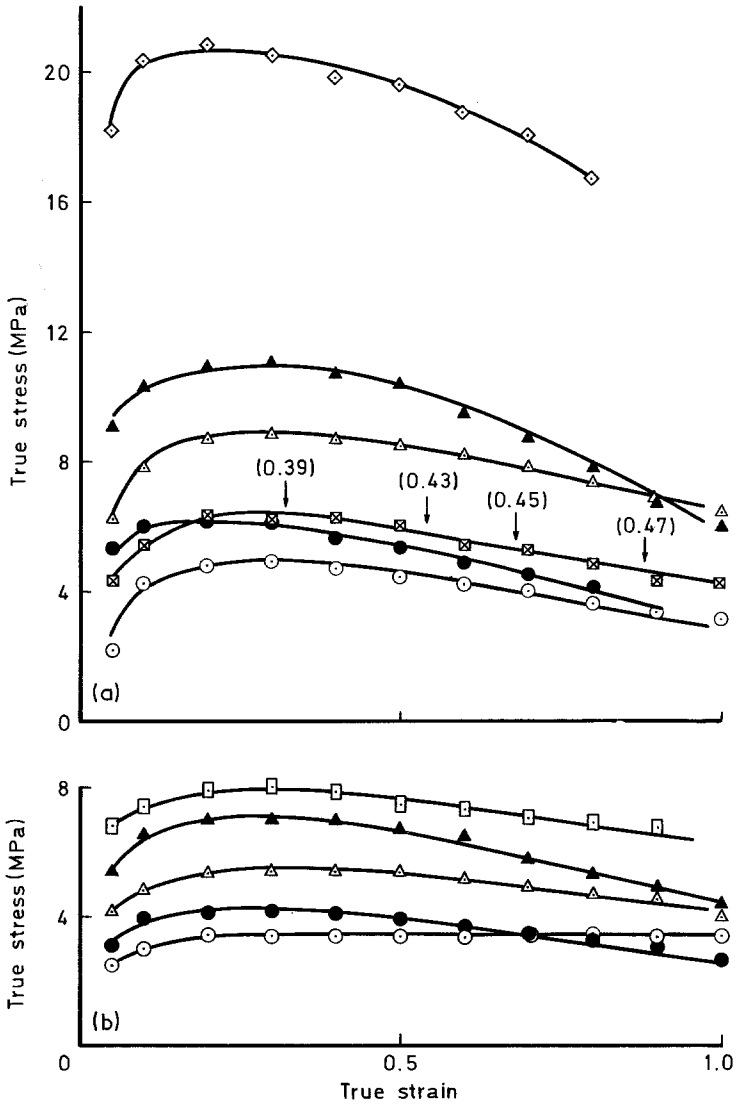


*Figure 3* Effect of initial strain rate, test-piece orientation and test temperature on true stress–true strain curves: (a) 500° C, (b) 540° C. Open symbols, L direction; closed symbols, T direction. Values of $\dot{\varepsilon}_I$ ($sec^{-1}$) as follows: (⊙, ●) $1.7 \times 10^{-4}$; (⊠) $3.4 \times 10^{-4}$; (△, ▲) $8.5 \times 10^{-4}$; (⊡) $1.7 \times 10^{-3}$; (◇) $1 \times 10^{-2}$.

direction at 500° C and a strain rate $3.4 \times 10^{-4}\ sec^{-1}$, when $m = 0.4$ to 0.45.

Transverse test pieces in all three alloys exhibited multiple necking. The effect of superplastic strain on the plastic strain ratio $R$ for longitudinal test pieces is shown in Fig. 5. For a given set of conditions $R$ increased with increasing strain, indicating that deformation became more isotropic. The greatest effect was obtained at the highest temperature and the fastest strain rate ($\dot{\varepsilon}_I = 8.5 \times 10^{-4}\ sec^{-1}$ at 540° C).

TABLE I Effect of temperature and initial strain rate on elongation

| Test temperature (° C) | Test direction | Initial strain rate ($sec^{-1}$) | Elongation (%) |
|---|---|---|---|
| 450 | L | $3.4 \times 10^{-4}$ | 130 |
| | | $1 \times 10^{-2}$ | 48 |
| | T | $8.5 \times 10^{-4}$ | 72 |
| 500 | L | $1.7 \times 10^{-4}$ | 233 |
| | | $3.4 \times 10^{-4}$ | 300* |
| | | $8.5 \times 10^{-4}$ | 248 |
| | | $1 \times 10^{-2}$ | 132 |
| | T | $1.7 \times 10^{-4}$ | 124† |
| | | $8.5 \times 10^{-4}$ | 152† |
| 540 | L | $1.7 \times 10^{-4}$ | 292* |
| | | $8.5 \times 10^{-4}$ | 280* |
| | T | $1.7 \times 10^{-4}$ | 228† |
| | | $8.5 \times 10^{-4}$ | 148† |

*Elongation without failure.
†Multiple necking along gauge length.

## 3.3. Room-temperature tensile tests

Test pieces superplastically deformed in the L direction exhibited uniform cross-sections throughout their gauge lengths. No further machining was therefore required in order to obtain valid tensile properties.

The tensile properties of heat-cycled and of superplastically deformed material are plotted against superplastic strain in Figs. 6 and 7. A small fall in strength was observed for material heat-cycled at 500° C (after heating for a time equivalent to $\varepsilon = 0.6$), whereas above a superplastic strain of only $\varepsilon = 0.3$ at $\dot{\varepsilon}_I = 3.4 \times 10^{-4}\ sec^{-1}$ there was a significant reduction in strength. The strength of heat-cycled material at 540° C decreased continuously with increasing time at temperature, and superplastically deformed material ($\dot{\varepsilon}_I = 1.7 \times 10^{-4}\ sec^{-1}$) showed a similar trend although the reduction in strength above $\varepsilon = 0.2$ was more marked.

The modulus appeared to be independent of superplastic strain. Both heat-cycled and strained material showed a slight increase in tensile elongation at times equivalent to about $\varepsilon = 0.5$ but decreased at higher equivalent times.

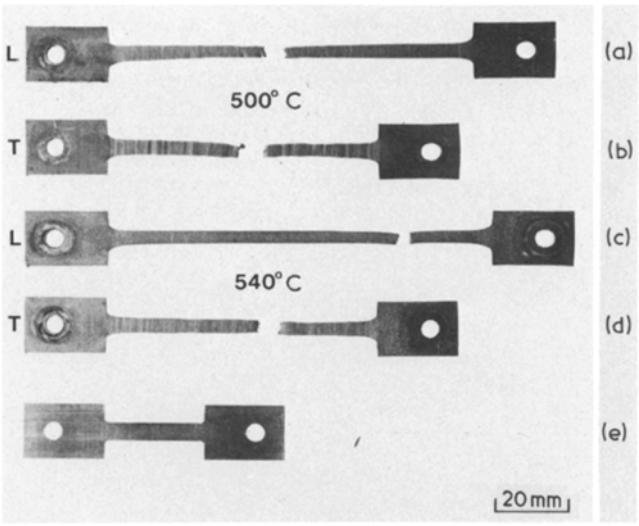


*Figure 4* Test pieces after superplastic strain. Elongations (a) 248%, (b) 152%, (c) 280%, (d) 148%, (e) undeformed.

### 3.4. Effect of deformation on microstructure

The effect of increasing strain on microstructure was studied after tests at 500° C and $\dot{\varepsilon}_I = 3.4 \times 10^{-4}\,sec^{-1}$ and at 540° C and $\dot{\varepsilon}_I = 1.7 \times 10^{-4}\,sec^{-1}$. Dynamic recrystallization was apparent after 0.49 strain at 500° C, but shear bands were still present and cavities tended to lie in these bands (Fig. 8a). After 1.46 strain an almost equiaxed grain structure was produced throughout the sheet section (Fig. 8b) with grain diameters $d_{MLI}$ of 5 to 10 $\mu$m. At the higher temperature of 540° C a larger grain size of 6 to 12 $\mu$m at $\varepsilon = 0.5$ and 11 to 17 $\mu$m at $\varepsilon = 1.43$ was obtained (Fig. 9b). Note that the undeformed test-piece head given the same heat cycle had a much finer microstructure (Fig. 9a).

The microstructures produced after deformation at fast strain rates $\dot{\varepsilon}_I = 1 \times 10^{-2}\,sec^{-1}$ and $1.7 \times 10^{-3}\,sec^{-1}$ at 500 and 540° C, respectively, consisted of regions of small grains together with regions of elongated grains.

At 500 and 540° C the void volume percentage of cavitation was less than 1% at $\varepsilon = 0.75$ (Figs. 6 and 7). With increasing strain the void volume increased linearly at rates of 6.6 and 4% void volume per unit of strain at 500° C ($\dot{\varepsilon} = 3.4 \times 10^{-4}\,sec^{-1}$) and 540° C ($\dot{\varepsilon} = 1.7 \times 10^{-4}\,sec^{-1}$), respectively. The void volumes measured after $\varepsilon = 1.4$ were 5.8% at 500° C and 3.7% at 540° C, respectively. Testing in the T direction at 540° C at $\dot{\varepsilon}_I = 1.7 \times 10^{-4}\,sec^{-1}$ produced a higher void volume than testing to the same strain in the L direction.

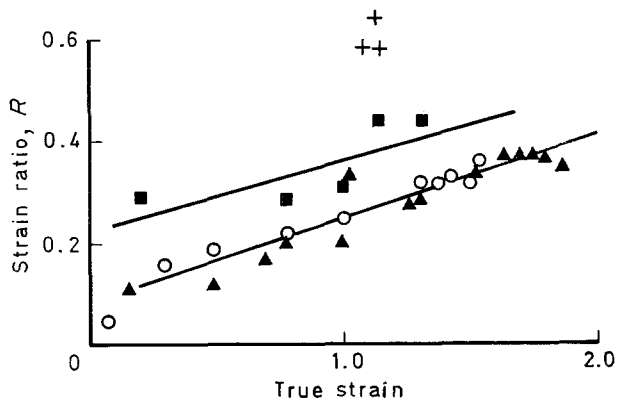


*Figure 5* Effect of superplastic strain on $R$ values for longitudinal test pieces. (■, ▲) 500° C; (○, +) 540° C. Values of $\dot{\varepsilon}_I$: (▲) $3.5 \times 10^{-4}$, (■) $8.5 \times 10^{-4}$, (○) $1.7 \times 10^{-4}$, (+) $8.5 \times 10^{-4}\,sec^{-1}$.

Metallography revealed that cavities nucleated at the grain boundaries and on shear bands, resulting in intergranular void formation and interlinkage of voids. The cavities were irregular in shape, variable in size and non-uniform in distribution (Fig. 10). At fast strain rates ($> 10^{-3}\,sec^{-1}$) the cavities tended to align in the tensile direction, whereas at lower strain rates this effect was not apparent. Cavities were not confined to the central region of the sheet, but were also present very close to the surface (Fig. 10).

### 3.5. Fractography

Longitudinal test pieces solution-treated at 500 and 540° C for various times before re-solution treatment and ageing exhibited 45° shear fractures when tensile-tested at room temperature. However, superplastically deformed test pieces after re-heat treatment and testing at room temperature showed a transition from 45° shear fracture after superplastic strains less than 0.7 to more normal fractures at greater strains (Fig. 11). This transition corresponded to a change in the fracture mode from transgranular to intergranular as the number of grain-boundary cavities increased (Fig. 12).

## 4. Discussion

All the test pieces exhibited greater superplastic elongations in the L direction than in the T direction; in the latter direction multiple necking was obtained. This anisotropy was probably caused by the absence of significant cross-rolling during processing, and was also revealed by the $R$ values measured after small strains ($< 0.2$); with increasing superplastic strain the $R$ values increased, indicating a change to more isotropic deformation (Fig. 5). A similar increase in $R$ value with increasing superplastic strain has been observed in titanium alloys [12].

The as-rolled sheet exhibited shear bands in the microstructure. Anneals at 500 and 540° C for up to 24 h did not completely remove the bands and did not lead to bulk recrystallization. However, a large recrystallized grain size was apparent in layers near the sheet

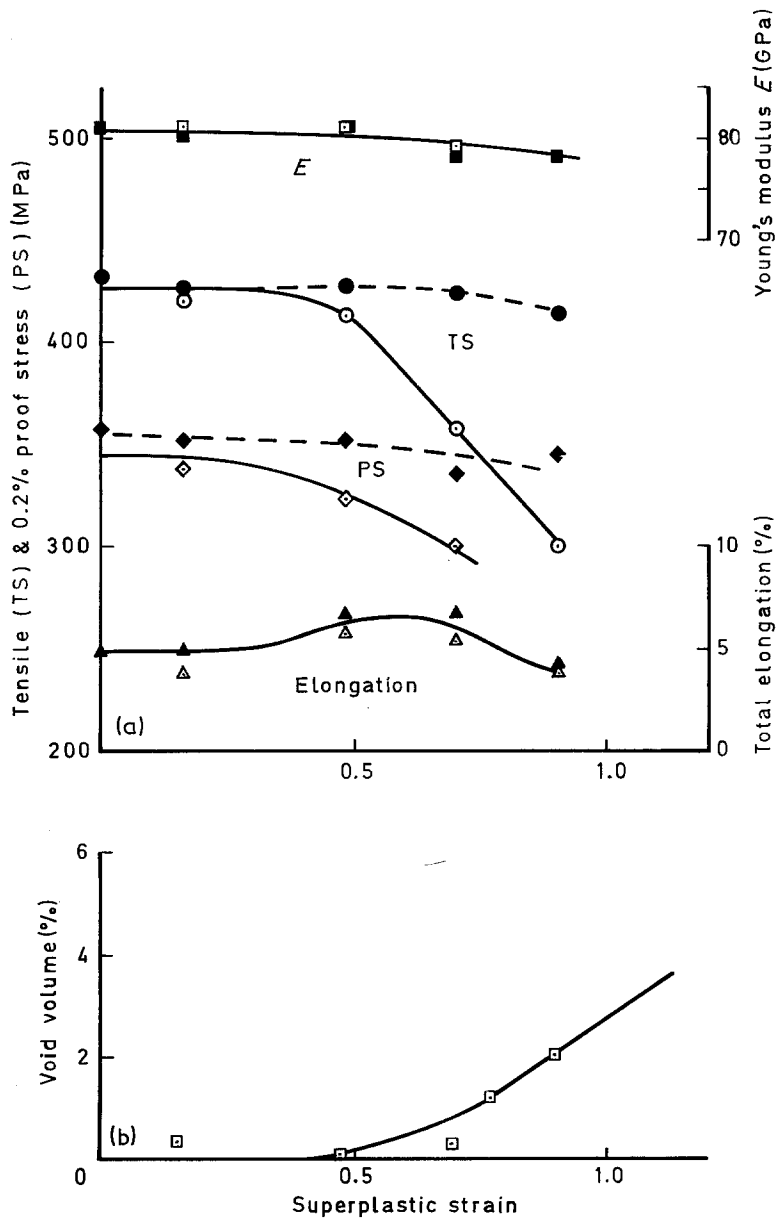


*Figure 6* Room-temperature tensile properties of sheet test pieces thermally cycled or superplastically deformed at 500° C and $\dot{\varepsilon}_1 = 3.4 \times 10^{-4}\,\text{sec}^{-1}$ and reheat treated: (a) tensile properties against superplastic strain, (b) void vol % against superplastic strain. Open symbols, superplastically deformed; closed symbols, thermally cycled for equivalent time.

surface associated with magnesium depletion. A denuded surface region was reported after heat treatment of an Al–Mg–Li (01420) alloy [13] at 450 and 500° C, and was attributed to the oxidation of magnesium and lithium. Lithium loss has been reported and studied in detail elsewhere [14]. A reduction in mechanical properties was attributed to lithium loss during processing of some American alloys at 482° C [15].

Dynamic recrystallization occurred during superplastic deformation, and with increasing strain an almost equiaxed grain microstructure developed throughout the sheet section. The maintenance of a fine grain size by dynamic recrystallization appears to be characteristic of the superplastic deformation in Al–6% Cu–0.5% Zr (Supral) and Al–Li alloys [16, 17]; recrystallization begins after about 0.5 strain. This behaviour differs from that of the Al–Zn–Mg alloys in which a fine grain size must be developed by thermomechanical processing (TMP) prior to superplastic forming [18] and is retained by suitable dispersed phases [19].

Prolonged solution heat-treatment times reduced the tensile strength of the Al–Li alloy, and superplastic strain caused a further decrease when significant cavitation occurred (Figs. 6 and 7). The reduction in strength above about 0.5 superplastic strain was therefore caused by a combination of recrystallization, grain growth, magnesium and lithium depletion and cavitation.

The low superplastic elongations ($\sim 300\%$) and low $m$ values ($\sim 0.43$) obtained in the present tests were much less than the values reported [16, 20] for TMP Al–Li alloys (800 to 1000% elongation, $m = 0.7$), but were typical of alloys with a cold-worked microstructure or of powder Al–Li alloys with a very small recrystallized grain size [21, 22]. The strain required for significant cavitation ($\sim 0.5$) was similar to that found for 7010 aluminium alloy cold-rolled before superplastic deformation [7] (Fig. 13) and within the scatter band for TMP Al–Zn–Mg alloys [8, 9, 21]. These results suggest that TMP may increase the total elongation but not greatly affect the onset of cavitation.

When the cold-rolled alloys were compared (Fig. 13) the rate of cavitation appeared to be greater in the

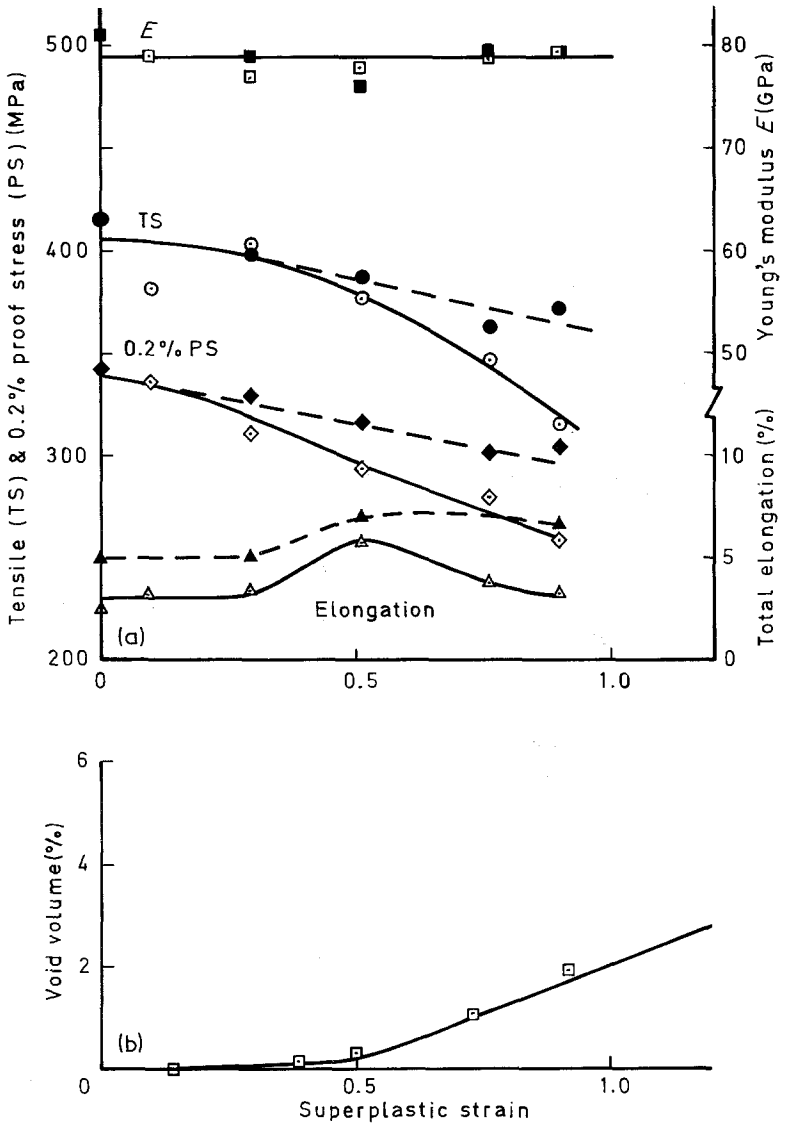


*Figure 7* Room-temperature tensile properties of sheet test pieces thermally cycled or superplastically deformed at 540° C and $\dot{\varepsilon}_1 = 1.7 \times 10^{-4}\,\text{sec}^{-1}$ and reheat treated: (a) tensile properties against superplastic strain, (b) void vol% against superplastic strain (540° C, $\dot{\varepsilon} = 1.7 \times 10^{-4}\,\text{sec}^{-1}$). Open symbols, superplastically deformed; closed symbols, thermally cycled for equivalent time.

7010 alloy than in the Al–Li–Cu alloy, even when the latter was deformed about a factor ten faster. Test data for TMP alloys have also indicated less cavitation in Al–Li alloys compared with Al–Zn–Mg alloys [21]. This may be a consequence of the greater mobility of the grain boundaries in the Al–Li alloys under conditions of dynamic recrystallization. There is evidence that cavitation can be suppressed by background pressure [23, 24], and the lower superplastic flow stress for Al–Li alloys compared with Al–Zn–Mg alloys indicates that a lower pressure will be required for Al–Li alloys [21].

Cavitation was evident very near the sheet surface in the softer coarse-grained layer (Fig. 10). This layer

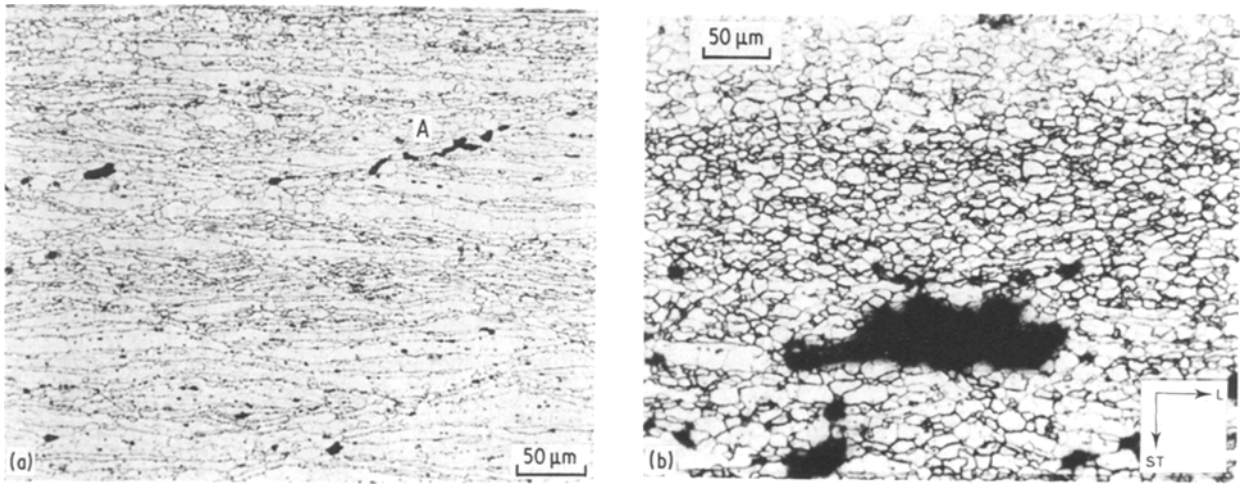


*Figure 8* Microstructure of longitudinal test piece after superplastic deformation at 500° C and $\dot{\varepsilon}_1 = 3.4 \times 10^{-4}\,\text{sec}^{-1}$: (a) $\varepsilon = 0.49$, (b) $\varepsilon = 1.46$.

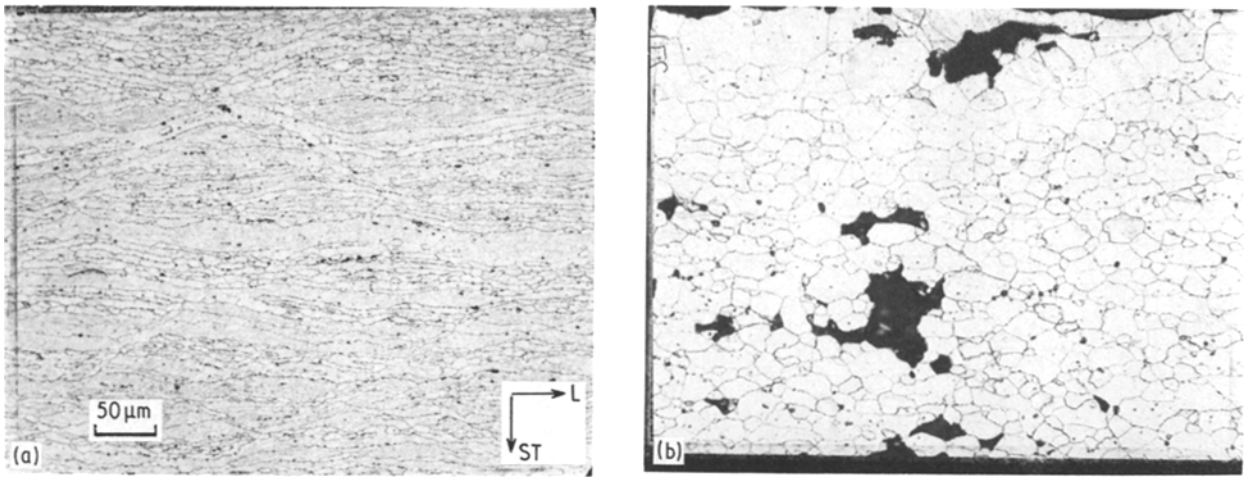


*Figure 9* Microstructure of longitudinal test piece after superplastic deformation at 540° C and $\dot{\varepsilon}_1 = 1.7 \times 10^{-4}$ sec$^{-1}$: (a) undeformed head of test piece, (b) $\varepsilon = 1.44$.

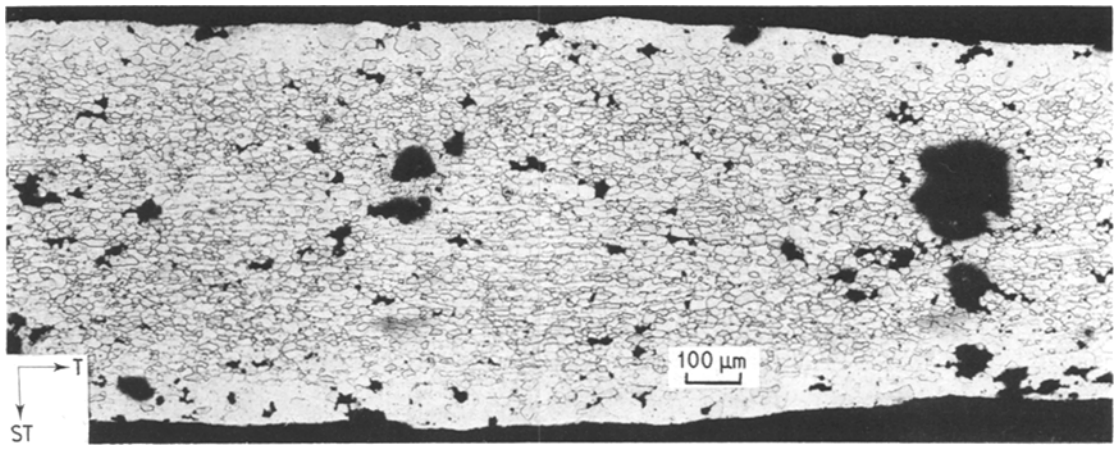


*Figure 10* Microstructure of transverse test piece after superplastic deformation at 540° C and $\dot{\varepsilon}_1 = 1.7 \times 10^{-4}$ sec$^{-1}$ to $\varepsilon = 1.14$.

might be considered to be equivalent to a clad layer. The results suggest that for clad sheet the protective effect of the cladding may be reduced after superplastic forming, since not only will the clad layer become thinner but cavities may provide corrosion paths to the base metal.

## 5. Conclusions

1. The maximum superplastic elongation obtained in cold-rolled and re-heat treated Al–Li–Cu alloy sheet was about 300% at 500° C and $3.4 \times 10^{-4}$ sec$^{-1}$ strain rate.

2. Longitudinal test pieces produced the largest elongations, and were more uniform in gauge width and thickness than transverse test pieces.

3. Dynamic recrystallization occurred during elevated temperature deformation, and at the strain rates and temperatures chosen an 8 to 15 $\mu$m diameter equiaxed grain structure was produced.

4. Solution treatment of the as-received sheet at 500

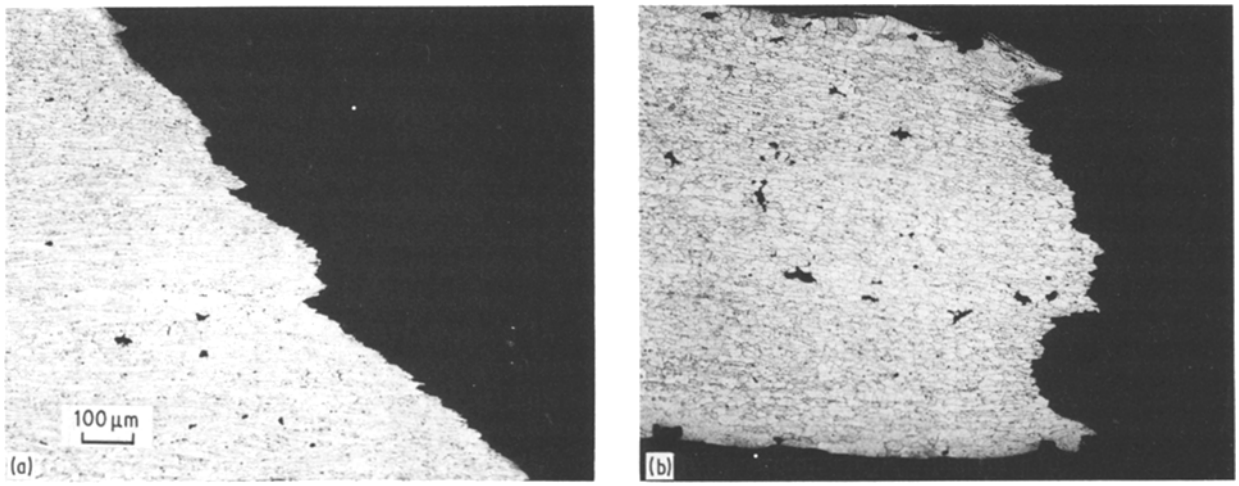


*Figure 11* Sections through room-temperature tensile fractures after superplastic deformation at 540° C and $\dot{\varepsilon}_1 = 1.7 \times 10^{-4}$ sec$^{-1}$ (longitudinal test piece): (a) $\varepsilon = 0.5$, (b) $\varepsilon = 0.76$, (c) $\varepsilon = 0.9$.

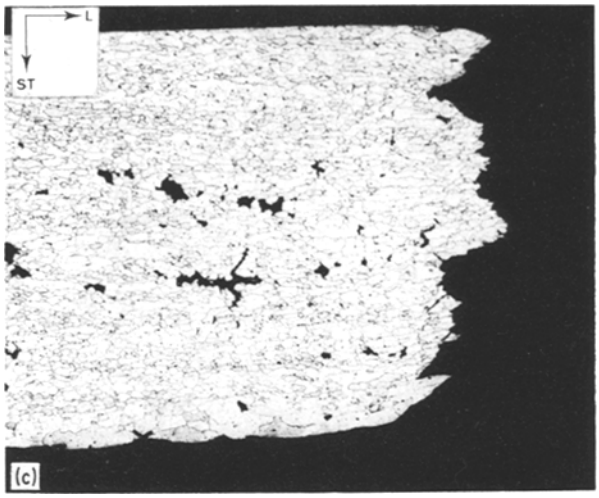


*Figure 11* Continued.

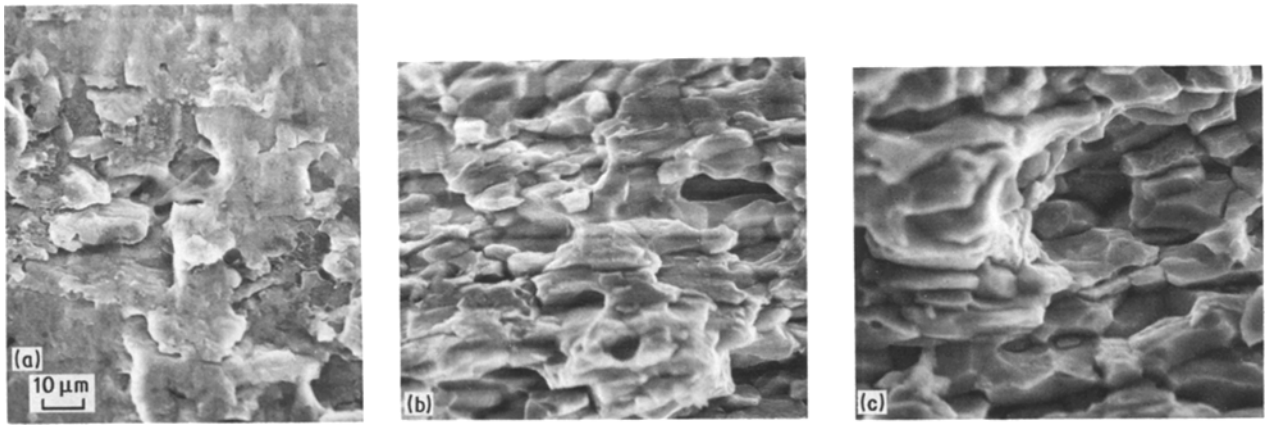


*Figure 12* Fracture surfaces of room-temperature fractures after superplastic deformation at 540° C and $\dot{\varepsilon}_1 = 1.7 \times 10^{-4}$ sec$^{-1}$ (longitudinal test piece): (a) $\varepsilon = 0.29$, (b) $\varepsilon = 0.76$, (c) $\varepsilon = 0.9$.

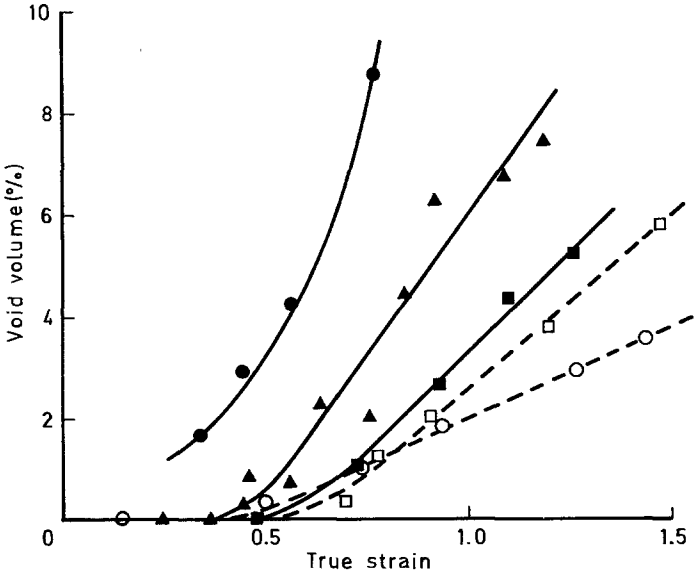


*Figure 13* Comparison of cavitation levels in cold-rolled Al–Zn–Mg alloy (7010) and in cold-rolled and heat-treated Al–Li–Cu alloy after superplastic deformation. (●, ▲, ■) Al–Zn–Mg–Cu at 500° C with (●) $\dot{\varepsilon}_1 = 2.8 \times 10^{-4}$ sec$^{-1}$, (▲) $\dot{\varepsilon}_1 = 2.8 \times 10^{-5}$ sec$^{-1}$, (■) $\dot{\varepsilon}_1 = 1.1 \times 10^{-5}$ sec$^{-1}$; (□) Al–Li–Cu–Mg at 500° C with $\dot{\varepsilon}_1 = 3.4 \times 10^{-4}$ sec$^{-1}$; (○) Al–Li–Cu–Mg with $\dot{\varepsilon}_1 = 1.7 \times 10^{-4}$ sec$^{-1}$.

and 540° C for times up to 24 h did not produce a fully recrystallized grain structure, but resulted in a surface layer denuded of magnesium and probably also of lithium.

5. Cavitaton was detected above 0.5 superplastic strain and increased linearly at 4 and 6 void vol % per unit strain at 540 and 500° C, respectively.

6. The onset of cavitation coincided with a reduction in the room-temperature strength, and a transition in the fracture mode from 45° transgranular shear to normal intergranular fracture.

## Acknowledgement

This paper is published with permission of the Royal

Aircraft Establishment. Copyright Controller HM Stationery Office, London, 1985.

## References


1. G. W. STACHER and D. E. WEISERT, "Concurrent superplastic forming/diffusion bonding of B–I components", Advanced Fabrication Processes AGARD Conference No. 256 NATO (1979).
2. S. J. SWADLING, "Fabrication of titanium at high temperatures" AGARD Conference No. 256 NATO (1979).
3. *Idem, Metallurgia* (March 1983) 106.
4. R. SAWLE, in Proceedings of Symposium on Superplastic forming of structural alloys, San Diego, June 1982, edited by N. E. Paton and C. H. Hamilton (Met. Soc. AIME) p. 307.
5. C. H. HAMILTON, Technical Report ARSCD–CR, 80001 (Rockwell International Science Center, California, 1980).
6. *Idem,* AFWAL RT–81–3051 (1981).
7. P. G. PARTRIDGE and A. J. SHAKESHEFF, RAE Technical Report 82117 (1982).
8. *Idem, J. Mater. Sci.* **20** (1985) 2408.
9. C. C. BAMPTON and J. W. EDINGTON, *J. Eng. Mater. Tech.* **105** (1983) 55.
10. C. J. PEEL, B. EVANS, C. A. BAKER, D. A. BENNETT, P. J. GREGSON and H. M. FLOWER, Proceedings of Second International Al–Li Conference, Monterey, California, April 1982, edited by E. A. Starke and T. H. Sanders (Met. Soc. AIME).
11. *Aluminium Ind.* **4** (1985) 6.
12. P. G. PARTRIDGE, A. W. BOWEN, C. D. INGLEBRECHT and D. S. MCDORMALD, in Proceedings of International Conference on Superplasticity, Grenoble, 1985 (Editions du CRNS, Paris, 1985) p. 10.
13. I. N. FRIDYLANDER, V. S. SANDLER, T. I. NIKOISKAYA, R. A. SAVINOV and I. N. ROSCHINA, *Russ. Metall. (Metally)* No. 2 (1978) 175.
14. D. J. FIELD and G. M. SCAMAN, Proceedings of Second International Al–Li Conference, Monterey, California, April 1982, edited by E. A. Starke and T. H. Sanders (Met. Soc. AIME).
15. D. J. CHELMAN, "Development of powder metallurgy Al–alloys for high temperature aircraft application, Phase II" ( NASA CR165965, November 1982).
16. R. GRIMES and W. S. MILLER, Proceedings of Second International Al–Li Conference, Monterey, California, April 1982 (Met. Soc. AIME).
17. E. NES, *Met. Sci.* (1979) 211.
18. J. A. WERT, N. E. PATON, C. H. HAMILTON and M. W. MAHONEY, *Met. Trans.* **12A** (1981) 1267.
19. C. C. BAMPTON and J. W. EDINGTON, *ibid.* **13A** (1982) 1721.
20. J. WADSWORTH, I. G. PALMER and D. D. CROOKS, *Scripta. Metall.* **17** (1983) 347.
21. R. J. LEDERICH, S. M. L. SASTRY and P. J. MESCHTER, *ibid.* **19** (1985) 177.
22. J. WADSWORTH and A. R. PELTON, *ibid.* **18** (1984) 387.
23. C. C. BAMPTON and R. RAJ, *Acta Metall.* **30** (1982) 2043.
24. C. C. BAMPTON, M. N. MAHONEY, C. H. HAMILTON, A. K. GHOSH and R. RAJ, *Met. Trans.* **14A** (1983) 1583.



*Received 7 May*
*and accepted 12 June 1985*